ELSEVIER

Thermochimica Acta 266 (1995) 213–229

thermochimica acta

Heat capacity and thermodynamic properties of millerite from 298.15 to 660 K and NiAs-type nickel(II) sulfide from 260 to 1000 K. Thermodynamics of the NiAs-type to millerite transition ☆

Fredrik Grønvold *, Svein Stølen

Department of Chemistry, University of Oslo, Postbox 1033 Blindern, 0315 Oslo, Norway

Abstract

The heat capacity of synthetic millerite, NiS, has been determined by adiabatic-shield calorimetry from 300 to 660 K where it transforms endothermally to the NiAs polytype (niccolite), $\Delta_{trs}H_m = 6591 \pm 50$ J mol^{-1}. The measurements were continued to 1000 K. The latter polytype is easily quenched and its heat capacity has been measured from 260 K, through the semimetal-to-metal transition at 270 K with $\Delta_{trs}H_m = 1394 \pm 20$ J mol^{-1}, and up to 340 K where it transforms exothermally to millerite with $\Delta_{trs}H_m$ (340 K) $= -5774 \pm 50$ J mol^{-1}. Thermodynamic function values for the NiS phases have been derived through integration of the present results and combining them with low-temperature results from the literature. The enthalpy increment for millerite at 298.15 K to the NiAs-type phase at 1000 K is 47140 J mol^{-1}, or about 7% higher than the drop-calorimetric results in the literature.

Keywords: Adiabatic calorimetry; Heat capacity; NiS; NiAs-type

1. Introduction

Nickel(II) sulfide exists in two well-characterized structural forms. The rhombohedral form, which is the form stable at ambient pressure and temperature [1–3], transforms into a quenchable phase with an NiAs-like structure [3] about 660 K [4–6].

* Corresponding author.

☆ Dedicated to Hiroshi Suga on the Occasion of his 65th Birthday.

SSDI 0040-6031(95)02447-6

While the low-temperature form, millerite, is closely stoichiometric, the NiAs-type phase, niccolite, has a rather large homogeneity range [5, 7 9]. The sulfur content influences the stability of the high-temperature phase, and a eutectoidal decomposition of $Ni_{1-x}S$ with $x = 0.09$ to millerite and Ni_3S_4 (polydymite) is observed at 555 K [5]. The high-temperature form is easily quenched and remains metastable at ambient temperature. Indications of a phase transformation in $Ni_{1-x}S$ in the temperature range 973 to 1073 K were, however, reported by Kullerud and Yund [5]. The presence of a $3a3a3c$ superstructure was subsequently observed [10]. Both Noda et al. [11] and Collin et al. [12] found an ordered $3a3a3c$ phase as well as a disordered phase, and independently proposed the composition $Ni_{17}S_{18}$ for the ordered phase. The structure of the phase has been refined by single-crystal X-ray work [13]. High-resolution electron microscopy on quenched non-stoichiometric nickel(II) sulfide by Black et al. [14] indicates the presence of an additional ordered $2a2anc$ phase and, hence, three different structural species occur within the non-stoichiometric region. The $3a3a3c$ structure is initially observed at temperatures above 1023 K. At lower temperatures, the $3a3a3c$ structure transforms to the disordered structure, which contains vacancies in all nickel layers.

Quenched metastable NiAs-type NiS undergoes a much studied semimetal-to-metal transition on heating to 265 K [15]. The presence of a small fraction of cation vacancies greatly influences the electronic properties of the phase and tends to stabilize the high-temperature metallic NiAs-type phase. The temperature of the semimetal-to-metal transition [15–19] decreases from 265 K for $Ni_{1.00}S$ to 53 K for $Ni_{0.968}S$ [19]. Even very small compositional fluctuations in the sample, hence, necessarily will give rise to somewhat diffuse or spread-out changes in the observed physical properties during the first-order transition [18].

As a result of the broad interest in the semimetal-to-metal transition, the thermophysical properties of the NiAs-type phase at low temperatures are fairly well known. Thus, determinations of elastic constants [19, 20], compressibility [21], thermal expansion [19], electrical properties [22], as well as low-temperature heat capacities have been reported. The heat capacity of millerite was measured by Weller and Kelley [23] over the temperature range 50–300 K. Heat capacity results for both metallic and semimetallic NiAs-type NiS were presented by Coey and Brusetti [18], by Brusetti et al. [19], and by Trahan and Goodrich [24] (from 30 to 330 K), and at very low temperatures (from 1 to 10 K) by Ohtani [25]. High-temperature enthalpy increments were first reported by Regnault [26], later by Tilden [27] at the beginning of this century, and more recently by Conard et al. [28], who also determined a value for the enthalpy of transition of NiS from millerite to NiAs-type structure. Their thoroughly calibrated DTA value, 6.4 ± 0.4 kJ mol^{-1}, was more than twice the value previously reported by Biltz et al. [4]. The latter value was largely confirmed by Ferrante, according to Mah and Pankratz [29], and preferred in phase diagram evaluations [9, 30, 31]. Dubusc et al. [6] did, however, obtain 5.86 ± 0.36 kJ mol^{-1}.

It appeared to us that the energetics of the millerite to NiAs-type transition, as well as the reverse exothermal transformation of the quenched phase to the stable phase with millerite structure, might be studied in our high-temperature adiabatic calorimeter. Step-wise heated adiabatic calorimeters are ideally suited both for studies of the true

heat capacity of metastable phases, and for studies of the thermodynamic and kinetic aspects of exothermal transformations [32].

We have measured the heat capacity of stoichiometric NiS from 260 K in both the quenched and stable state. Furthermore, with knowledge of the heat capacity of both phases from low temperatures and interpolating the heat capacity for the metastable phase over the range in which it is not easily measured, a complete thermodynamic cycle is obtained. This cycle relates the two phases through their Gibbs energy or enthalpy difference at 0 K.

The present study is part of an extensive study on the thermodynamics of the nickel–sulfur system [33–35].

2. Experimental

2.1. Synthesis and structural characterization

Three samples of nickel(II) sulfide were prepared directly from the elements; nickel as 5 mm diameter rods (> 99.998 mass%) for two of the samples and pure sulfur crystals (99.9999 mass%) from Koch-Light Laboratories, Colnbrook, England. For the third sample, hydrogen-reduced nickel(II) oxide powder (BDH, low in Co and Fe) was used. Stoichiometric amounts of the elements were heated in an evacuated, sealed vitreous silica tube, constricted at the middle by a smaller diameter tube. Nickel was placed in one part of the tube, sulfur in the other, and the tube was put into a reclining tube furnace with the sulfur-containing compartment protruding. The nickel was heated to 870 K and the sulfur was allowed to melt and react with the nickel in the hotter part of the tube. After 2 days, most of the sulfur had reacted with the nickel. A heating pad was then wound around the protruding part of the silica tube for the remaining sulfur to be brought into reaction. This was accomplished overnight. The empty half of the silica tube was sealed off and removed. Sample A was then equilibrated at 1270 K for 3 h and cooled with the furnace. It was then finely crushed and transferred to the calorimetric ampoule. Samples B and C were prepared in similar ways, but subsequently annealed at 770 K for 7 days and cooled with the furnace.

Room-temperature X-ray powder photographs were taken using the Guinier technique with Cu $K\alpha_1$ radiation. Unit-cell dimensions were derived by applying a least-squares routine. The derived lattice constants are presented in Table 1 together with earlier published values. For millerite, they agree best with those for the sulfur-rich sample reported by Lundqvist [36]. The less rapid quenching for the NiAs-type calorimetric sample is reflected in its smaller lattice constants compared to those for a smaller sample quenched from 770 K.

2.2. Calorimetric technique

The high-temperature calorimetric apparatus and measuring technique have been described earlier [40, 41], along with results obtained for the heat capacity of a standard sample of α-Al_2O_3. The calorimeter is heated intermittently, and surrounded by

Table 1
Lattice constants of the NiS phases

Investigator	Millerite	a/pm	c/pm	Ref.
Lundqvist	Ni-rich	961.6	315.1	[36]
Lundqvist	S-rich	960.6	315.1	[36]
Lundqvist	Mineral	961.0	315.1	[36]
Kullerud and Yund	Stoichiometric	961.6	315.2	[5]
Kullerud and Yund	S-rich	961.5	315.1	[5]
Dubusc et al.		961.5(4)	315.1(2)	[6]
Present	Stoichiometric	960.7(6)	315.1(4)	

Investigator	NiAs-type	Quenched from	a/pm	c/pm	Ref.
Lundqvist	Ni-rich		343.5	535.1	[36]
Lundqvist	S-rich		342.7	535.6	[36]
Laffitte	Ni-rich		343.92	534.84	[7]
Laffitte	S-rich		343.2	513.3	[7]
Kullerud and Yund	NiS	973 K	343.8(1)	534.8(1)	[5]
Kullerud and Yund	$Ni_{0.971}S$	873 K	342.3(1)	532.5(1)	[5]
Kullerud and Yund	$Ni_{0.950}S$	873 K	343.1(1)	532.5(1)	[5]
Kullerud and Yund	$Ni_{0.931}S$	933 K	342.6(1)	532.2(1)	[5]
Kullerud and Yund	$Ni_{0.916}S$	973 K	342.8(1)	531.5(1)	[5]
Trahan et al.	NiS		343.95(2)	535.14(7)	[37]
McWhan et al.			343.98(3)	534.82(5)	[38]
Berthelemy et al.			344.1(1)	535.4(1)	[39]
Brusetti et al.	NiS		344.7	535.0	[19]
Dubusc et al.			343.92(5)	534.84(9)	[6]
Black et al.	NiS		344.8(2)	535.9(3)	[14]
Black et al.	$Ni_{0.95}S$		342.9(2)	532.5(7)	[14]
Present	NiS[a]		343.45(3)	533.98(7)	
Present	NiS	770 K	344.04(3)	535.39(6)	

[a] Calorimetric sample.

electrically heated, electronically controlled adiabatic silver shields. There is a heated guard system, also of solver, outside the shields and the whole assembly is placed in a vertical tube furnace. The temperature differences between corresponding parts of the calorimeter and shield are measured by means of Pt–(Pt + 10 mass% Rh) thermopiles. The amplified signals are recorded and also used for automatic control of the shield heaters to maintain quasi-adiabatic conditions during input and drift periods. The temperature of the guard body is kept 0.4 K below that of the shield, while the temperature of the furnace is kept 10 K lower to secure satisfactory operation of the control units. Sub-ambient conditions are obtained by submerging the calorimeter in a water/ice/NaCl mixture.

The mass of the sample used in the experiments was about 125 g for samples A and B, and 93 g for C. The samples were enclosed in evacuated and sealed vitreous silica tubes of about 50 cm^3 volume, tightly fitted into the silver calorimeter. A central well in the

tube served for the heater and the platinum resistance thermometer which was calibrated locally, at the ice, steam, tin, zinc, and antimony points. The thermometer resistance was measured with an automatically balancing ASL18 a.c. bridge, operated by a Hewlett-Packard 9835A computer in the later series of measurement. Temperatures are judged to correspond with IPTS-68 to within 0.05 K from 300 to 900 K, and within 0.1 K at 1000 K, whereas the precision in the temperature determination is within 0.00002 K. The energy inputs from a constant-current supply are measured with a Hewlett-Packard digital voltmeter with an accuracy of 0.025%.

The heat capacity of the calorimeter plus empty sample container was determined in a separate series of experiments with a standard deviation of single measurements from the smoothed heat capacity curve of about 0.15%. The heat capacity of the empty calorimeter represented approximately 60% of the total heat capacity. Small corrections were applied for differences in mass of the empty and full vitreous silica containers and for the "zero" drift of the calorimeter.

The computer-operated experiments are started after obtaining a low and steady instrumental temperature drift (less than 1 mK per min over long periods). Under ordinary conditions, i.e. when no phase transformation takes place in the sample, the calorimeter temperature reaches its new equilibrium value about 30–40 min after the end of the input in the ambient temperature range, and within 10 min at 1000 K. In transformation regions, longer equilibration intervals are used (up to several days, see e.g. Ref. [42]). The standard deviation of a single measurement from the smoothed heat capacity curve is generally of the order of 0.3% when no phase reactions occur in the sample, whereas the uncertainty in the heat capacity values is judged to be within 0.3%, and the enthalpy and entropy increments within 0.2%.

3. Results and discussion

3.1. Heat capacities

Results of the heat capacity determinations are presented in chronological order for one mole of NiS in Table 2 and graphically in Fig. 1. The approximate temperature increments used in the determinations can usually be inferred from the adjacent mean temperatures given in the table.

The heat capacity of the millerite-type phase rises smoothly with temperature up to 600 K. A small heat capacity peak at around 610 K is followed by a further rise and transitional enthalpy absorption at about 660 K, where the phase change to the NiAs-type structure occurs. On further heating, the heat capacity rises smoothly up to around 900 K. Above this temperature, a significant increase is again observed. This is presumably related to the start of exsolution of the $Ni_{3\pm x}S_2$ phase as the nickel-rich limit of the NiS phase is already more sulfur-rich at this temperature, see below. When this NiAs-type phase is quenched, one first sees the semimetal-to-metal transition at about 270 K. Then at about 330 K, a positive temperature drift rate relative to the instrumental one is observed in the equilibration period. This reflects the beginning of reversion to the stable phase with millerite structure.

Table 2
Molar heat capacities of NiS, $R = 8.3145$ J K^{-1} mol^{-1}

T/K	$C_{p,m}/R$	T/K	$C_{p,m}/R$	T/K	$C_{p,m}/R$	T/K	$C_{p,m}/R$	T/K	$C_{p,m}/R$	T/K	$C_{p,m}/R$
					M(NiS) = 90.759 g mol^{-1}						
Sample A		512.53	6.3696	259.50	5.5517	378.15	5.9847	330.43	6.1122	758.75	7.2452
Series I		522.17	6.4177	Detn. E		386.20	5.9944	336.96	6.1339	766.14	7.3077
589.32	6.6943	531.83	6.4610	285.15	5.9751	394.39	6.0497	Detn. H		773.51	7.3582
598.89	6.7232	541.47	6.5043	291.69	5.9583	402.56	6.0834	413.50	6.1074	780.88	7.2285
Detn. A		551.16	6.5139	304.70	6.0016	410.74	6.1050	Series VII		788.33	7.3919
681.74	7.3703	560.83	6.5500	311.18	6.0184	418.90	6.1291	260.96	5.4122	795.80	7.3943
Sample B		570.52	6.5957	317.62	6.0449	427.06	6.1483	267.61	5.8332	803.28	7.3871
Series II		580.24	6.6486	324.04	6.0665	435.23	6.1844	274.17	5.7081	824.87	7.4809
302.29	5.7057	589.94	6.6703	330.45	6.0858	443.42	6.1964	280.81	5.5566	832.42	7.4857
313.00	5.7298	599.68	6.7088	336.84	6.1218	451.60	6.2253	289.17	5.5999	839.99	7.5290
322.95	5.7779	Detn. B		Detn. F		468.02	6.2421	299.19	5.6576	843.22	7.4641
332.81	5.8212	687.17	7.1634	409.10	6.0785	476.24	6.2493	309.22	5.7177	851.83	7.6012
342.61	5.8621	695.17	7.1682	417.28	6.0112	484.47	6.2950	319.22	5.7658	861.35	7.5964
352.35	5.9029	704.84	7.2187	425.48	6.0497	492.72	6.3215	329.21	5.8115	870.90	7.6349
362.07	5.9246	714.73	7.2572	433.67	6.0665	500.98	6.3431	339.20	5.8500	880.50	7.6108
371.72	5.9751	723.41	7.3149	Series V		509.23	6.3648	349.21	5.8885	890.08	7.7287
381.42	6.0112	728.82	7.2668	260.87	5.4459	517.51	6.3912	359.22	5.9294	899.68	7.7046
392.10	6.0256	Series III		269.60	5.5084	525.73	6.4778	369.24	5.9679	909.28	7.7311
401.70	6.0569	260.08	5.6792	278.25	5.5566	533.98	6.5067	379.29	6.0016	901.69	7.7599
411.29	6.0761	Detn. C		286.98	5.6263	542.22	6.5187	389.35	6.0377	911.30	7.8177
420.88	6.1026	286.49	5.9535	295.61	5.6504	Series VI		399.43	6.0665	920.90	7.9788
430.52	6.1531	293.01	5.9679	304.02	5.6913	260.99	5.5710	409.57	6.0930	930.46	8.1376
440.11	6.1796	299.49	5.9919	312.40	5.7177	Detn. G		419.75	6.1242	939.97	8.2290
449.71	6.2132	305.94	6.0401	320.72	5.7634	285.07	5.8909	Sample C		949.51	8.3781
458.59	6.2229	312.36	6.0761	329.01	5.7923	291.53	5.9246	Series VIII		959.08	8.3180
466.72	6.2686	318.75	6.1098	337.27	5.8163	298.00	5.9559	690.93	7.1634	968.68	8.4888
474.84	6.2758	325.13	6.1291	345.50	5.8524	304.46	5.9895	722.11	7.1778	979.48	8.5177
483.67	6.3143	331.49	6.1555	353.70	5.8837	310.92	6.0232	729.74	7.2764	991.45	8.7245
493.28	6.3167	Detn. D		361.87	5.9198	317.42	6.0858	737.16	7.2404		
502.91	6.3504	Series IV		370.02	5.9559	323.93	6.0858	753.04	7.3077		

Three drop-calorimetric results by Tilden [27] have previously served as the basis for a linear heat capacity equation by Kelley [43] (dotted line in Fig. 1) which gives slightly lower values for millerite than observed here, see Fig. 1, while the mean heat capacity over the region 285–371 K reported by Regnault [26] is less than 1% higher. Slightly higher results were obtained for millerite in the unpublished work by Ferrante, as presented by Mah and Pankratz [29] (broken line), while the linear increase for the NiAs-type phase falls partly above and partly below. The linear enthalpy increase with temperature observed in the drop-calorimetric work of Conard et al. [28] (solid line) gave $C_{p,m} = 50.58$ J K mol^{-1} for millerite over the region 298.15–620 K, and $C_{p,m} = 57.33$ J K mol^{-1} for the NiAs-type NiS from 670 to 1000 K. The latter value falls far below the present results, see Fig. 1.

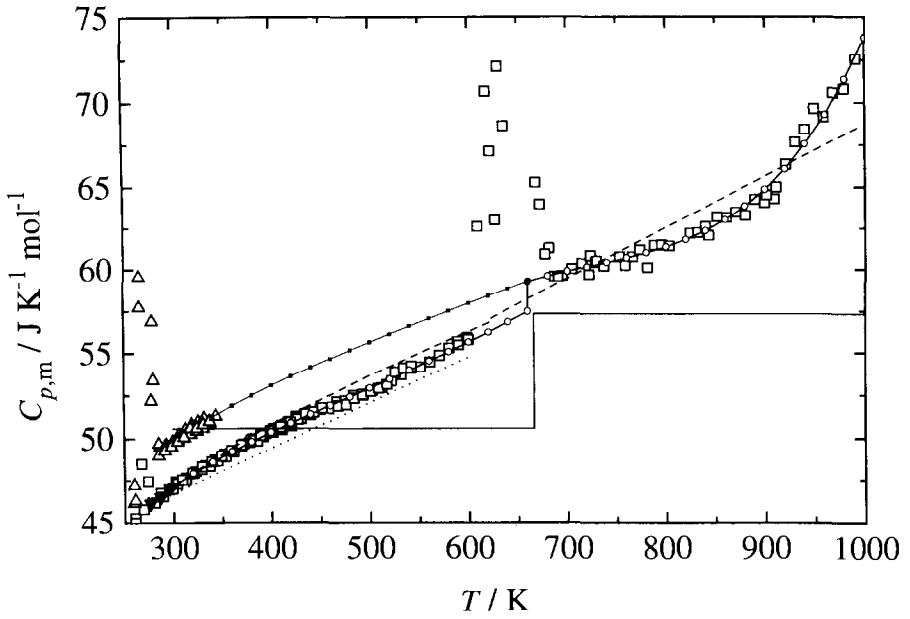

Fig. 1. Heat capacity of nickel(II) sulfide: Δ, present results for the metastable NiAs-type phase; □, present results for millerite up to about 660 K and for the NiAs-type above; ▼, results for millerite by Weller and Kelley [23]; ···, results by Tilden [27] as evaluated by Kelley [43]; – – –, results by Ferrante according to Mah and Pankratz [29]; —, results by Conard et al. [28]. The solid line with black symbols represents the estimated heat capacity for the NiAs-type phase in the temperature region where it is unstable, whereas the solid line with open symbols shows the polynomial representation of the heat capacity in the present calculation of the thermodynamic properties.

3.2. Transitions

3.2.1. The semimetal-to-metal transition in metastable NiAs-type NiS

The presently observed heat capacity peak reflecting the first-order transition from semimetal to metal, shown in Fig. 2, is somewhat broad. This departure from first-order behavior can be understood by taking into consideration that the transition temperature is lowered by 30 K for $Ni_{0.994}S$ compared to stoichiometric NiS [19]. Thus, even a very slight compositional variation is expected to cause a significant change in the transition temperature. The broadness of the heat capacity peak presumably reflects that the sample is composed of crystallites with slightly differing composition and strain. Individual crystallites have been shown [18] to transform independently and thereby cause discrete, very sharp heat capacity spikes as the temperature is changed.

The presently measured transitional enthalpy increments are given in Table 3, while the total enthalpy of transition is listed in Table 4 together with earlier reported values for stoichiometric NiS. The values depend slightly on the non-transitional reference heat capacities, see Fig. 2. Transitional enthalpy values were also calculated by Koehler and White [44] from an earlier reported value for the discontinuous volume change

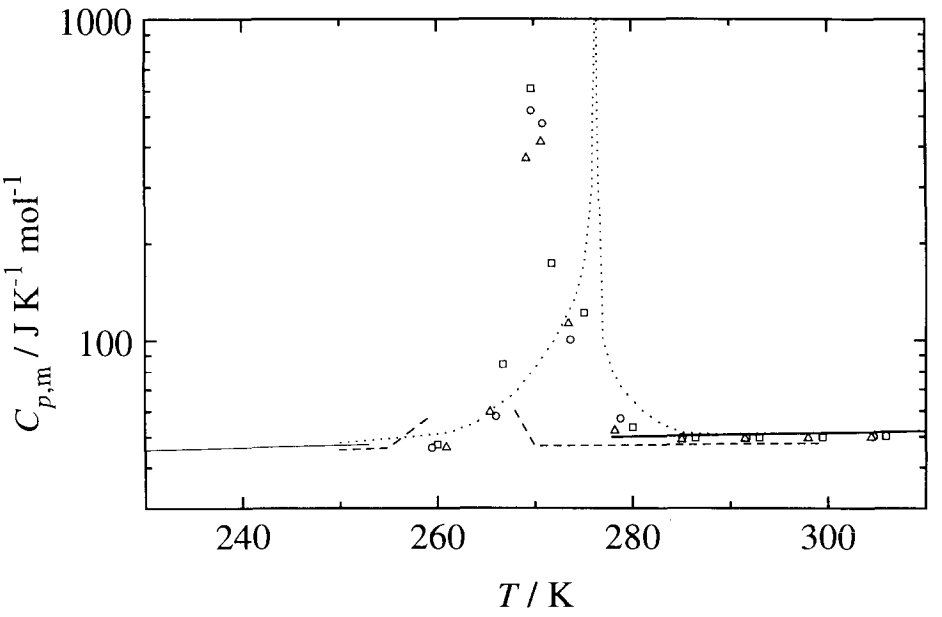

Fig. 2. Heat capacity of the metastable NiAs-type NiS in the semimetal-to-metal transition region: Δ, □, and ○, present results, detns. C, D, and G; ···, results in transition region by Trahan and Goodrich [24]; —, equations by Trahan and Goodrich [24]; – – –, results by Coey and Brusetti [18].

during the transition [45] and two values for the temperature–pressure relation [19,38] of the transition.

3.2.2. The millerite-toNiAs-type transition

Details of the heat capacity in the transitional region for two series of measurements on two different samples are given in Fig. 3. The main heat capacity effect with a maximum at around 660 K, observed for both specimens, is due to the formation of NiAs-type NiS. A heat-capacity rise in the region 605–615 K is followed by a decrease and a new increase. The effect is more pronounced for sample A (detn. A) which was cooled with the furnace from 1270 K than for sample B (detn. B), which had been subject to long-term annealing at 770 K as a last step in the preparation. The fractional enthalpy increments of the transition are listed in Table 3, with practically the same integral value for the two series for the enthalpy of transition of millerite to the NiAs-type NiS. Thus, the somewhat different pretransitional behavior appears to be caused by subtle minor reactions, see below.

The mean value obtained for the enthalpy of transition is listed in Table 5 together with earlier reported values. The value reported by Conard et al. [28] using quantitative DTA is in quite good accord with the one obtained here, as is the result by Dubusc et al. [6]. It is more than twice the highest value obtained in DTA heating experiments by Biltz et al. [4] and in the drop-calorimetric experiments by Ferrante, as reported by

Table 3
Molar enthalpies of transition of nickel(II) sulfide

$\langle T \rangle$/K	ΔT/K	$C_{p,m}$/(J K^{-1} mol^{-1})	$C_{pn.l}$/(J K^{-1} mol^{-1})	Δt/min	$\Delta_{trs}H$/(J mol^{-1})	T_{fin}/K
			M(NiS) = 90.759 g mol^{-1}			
			Metastable semimetallic to metallic NiAs-type			
Detn. C						264.2821
266.759	4.9545	84.16	46.84	88	184.9	269.2366
269.724	0.9741	607.1	47.32	90	545.2	279.2107
271.700	2.9781	173.2	48.66	88	370.8	273.1888
275.055	3.7333	121.4	48.78	80	271.0	276.9221
280.073	6.3027	53.40	49.00	59	27.7	283.2248
					1399.6	
Detn. E						262.9805
266.073	6.1857	57.74	46.80	88	67.7	269.1662
269.725	1.1176	519.4	47.38	87	527.5	270.2838
270.903	1.2384	474.4	48.60	89	527.3	271.5222
273.661	4.2783	100.1	48.72	89	220.0	275.8001
278.843	6.0863	56.90	48.96	89	48.3	281.8865
					1390.8	
Detn. G						262.47032
265.439	5.93668	59.56	46.76	67	76.0	268.40700
269.202	1.58962	367.5	46.92	67	509.5	269.99662
270.723	1.45341	412.9	48.60	89	529.5	271.45003
273.456	4.01220	112.4	48.72	189	255.6	275.46223
278.234	6.33834	52.20	48.96	188	20.5	281.00570
					1391.1	
				Mean value	1393.8	
			Millerite to NiAs-type			
Detn. A						603.716
607.351	7.270	89.36	55.80	71	244.0	610.986
614.357	6.741	102.0	56.05	68	309.7	617.727
622.115	8.776	67.12	56.23	83	95.6	626.503
630.720	8.434	72.12	56.54	77	131.4	634.558
638.748	7.621	85.54	56.80	68	219.0	648.558
645.754	6.392	111.9	57.02	97	350.7	648.950
651.471	5.042	155.5	57.20	209	495.5	653.992
654.649	1.313	737.0	57.29	380	892.5	655.305
655.373	0.136	7540	57.30	499	1017.4	655.441
655.610	0.337	3014	57.31	609	996.2	655.778
658.015	4.473	413.4	57.50	2462	1591.9	660.251
664.085	7.668	86.08	59.32	248	205.2	667.919
672.500	9.170	63.96	59.46	76	41.2	677.089
					6590.3	
Detn. B						604.5398
609.144	9.2087	62.60	55.90	103	61.7	613.7485
618.076	8.6546	71.08	56.17	97	129.0	622.4031
627.059	9.3120	63.00	56.44	98	61.1	631.7151
636.187	8.9430	68.64	56.72	98	106.6	640.6581
644.462	7.6077	92.08	56.97	102	267.1	648.2658
650.393	4.2547	214.2	57.15	105	668.4	652.5205
658.091	11.1414	527.5	57.96	1238	5231.3	663.6619
668.314	9.3044	65.26	59.39	95	54.6	672.9663
677.605	9.2777	60.90	59.54	212	12.6	682.2440
					6592.4	
				Mean value	6591.3	

Table 4
Molar transitional enthalpies for nickel(II) sulfide

T_{trs}/K	$\Delta_{trs}H_m$/J mol^{-1}	Authors
	NiAs-type; non-metal to metal	
270	1394 ± 20	Present
276.4	1383	Trahan and Goodrich [24]
265	1409 ± 42	Coey and Brusetti [18]
267	1180	Koehler and White [44]
228	810	Koehler and White [44]
210	630[a]	Koehler and White [44]
230	880[a]	Koehler and White [44]
	Millerite to NiAs-type	
660	6591 ± 50	Present
669	2600	Biltz et al. [4]
652	6444	Conard et al. [28]
667	5860 ± 360	Dubusc et al. [6]

[a] Calculated from ΔV[45] and dp/dt [21, 38] results using the Clapeyron relation.

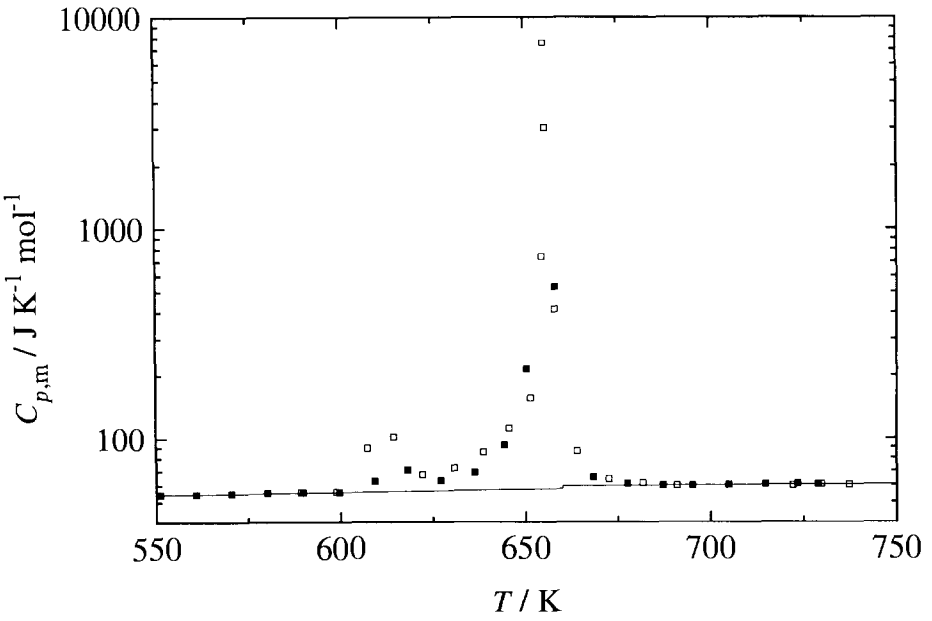

Fig. 3. Heat capacity of nickel(II) sulfide in the millerite-to-NiAs-type transition region: □ and ■, present results, dctns. A and B; —, non-transitional heat capacity.

Mah and Pankratz [29]. The latter values were used in the thermodynamic evaluation of the Ni + S system by Lin et al. [9]. The value by Conard et al. [28] was considered to be inconsistent with their phase diagram evaluation as it led to an incorrect temperature dependence for the Gibbs energy of formation for Ni_3S_4. The present confirmation

Table 5
Molar thermodynamic properties of nickel(II) sulfide

T/K	$C_{p,m}$/ (J K^{-1} mol^{-1})	$\Delta_0^T H_m$/ (J mol^{-1})	$\Delta_0^T S_m$/ (J K^{-1} mol^{-1})	Φ_m/ (J K^{-1} mol^{-1})	T/K	$C_{p,m}$/ (J K^{-1} mol^{-1})	$\Delta_0^T H_m$/ (J mol^{-1})	$\Delta_0^T S_m$/ (J K^{-1} mol^{-1})	Φ_m/ (J K^{-1} mol^{-1})
				M(NiS) = 90.759 g mol^{-1}					
Millerite					NiAs-type				
298.15	47.08	8577	52.96	24.19	660.00	59.26	34126	104.18	52.47
300.00	47.16	8664	53.25	24.37	680.00	59.58	35314	105.95	54.02
320.00	47.92	9615	56.32	26.27	700.00	59.87	36509	107.68	55.53
340.00	48.60	10581	59.25	28.13	720.00	60.14	37709	109.37	57.00
360.00	49.23	11559	62.04	29.93	740.00	60.40	38914	111.03	58.44
380.00	49.81	12549	64.72	31.69	760.00	60.69	40125	112.64	59.84
400.00	50.36	13551	67.29	33.41	780.00	61.00	41342	114.22	61.22
420.00	50.89	14564	69.76	35.08	800.00	61.36	42565	115.77	62.56
440.00	51.41	15587	72.14	36.71	820.00	61.81	43797	117.29	63.88
460.00	51.92	16620	74.43	38.30	840.00	62.35	45038	118.79	65.17
480.00	52.42	17663	76.65	39.86	860.00	63.02	46292	120.26	66.43
500.00	52.93	18717	78.80	41.37	880.00	63.84	47560	121.72	67.67
520.00	53.45	19781	80.89	42.85	900.00	64.85	48847	123.16	68.89
540.00	53.98	20855	82.92	44.30	920.00	66.08	50156	124.60	70.08
560.00	54.51	21940	84.89	45.71	940.00	67.55	51491	126.04	71.26
580.00	55.07	23035	86.81	47.10	960.00	69.30	52859	127.48	72.42
600.00	55.64	24142	88.69	48.45	980.00	71.37	54266	128.93	73.56
620.00	56.23	25261	90.52	49.78	1000.00	73.79	55717	130.39	74.68
640.00	56.83	26392	92.32	51.08					
660.00	57.47	27535	94.08	52.36					

of the value by Conard et al. [28], hence, indicates that the Gibbs energy of formation equations in the phase diagram evaluation by Lin et al. [9] are somewhat in error for NiS and the more sulfur-rich phases.

Previous investigators disagree as to the NiAs-type phase being not only nickel deficient but also containing excess nickel. Thus Rosenqvist [46] reported the homogeneity range to extend from $x_S = 0.498$–0.514 in the temperature region 670–780 K, while according to Kullerud and Yund [5] the NiAs-type phase is stoichiometric at 870 K in equilibrium with the $Ni_{3\pm x}S_2$ phase. On heating to 970 K, a very small amount of the $Ni_{3\pm x}S_2$ phase was found to exsolve from NiS, but the deviation from stoichiometry was estimated to be within 0.05 wt% at 1070 K, i.e. $Ni_{0.9986}S$. The deviation from stoichiometry becomes more pronounced above this temperature, but the available results diverge, see Fig. 4. The results presented by Rau [8] are internally inconsistent as the ordinate on his fig. 4, which indicates that the NiAs-type phase contains excess nickel below 1038 K, is at variance with the results in Fig. 3 and the phase diagram in Fig. 4. According to the two latter figures the limiting phase composition is $Ni_{0.997}S$ in the 850 K region.

In the present study, no extra heat effect was observed at about 850 K. The NiAs-type NiS appears to be free from measurable amounts of Ni_3S_2 phase and thus includes the

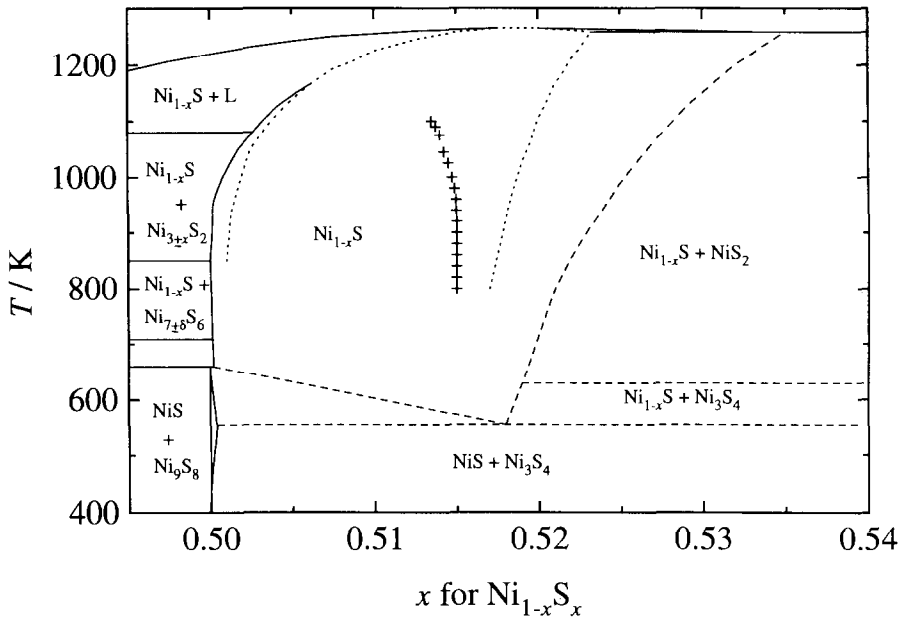

Fig. 4. Section of the Ni + S phase diagram in the NiS region: ···, phase limits by Rau [8]; – – –, phase limits by Kullerud and Yund [5]; + +, sulfur-rich phase limit for NiAs-type $Ni_{1-x}S$ phase by Laffitte [7]; ——, transition temperatures for more nickel-rich phases by Stølen et al. [34] and liquidus line by Lin et al. [9].

stoichiometric ratio at this temperature. The present heat capacity measurements do, however, show an increasing rise above 900 K, which presumably is related to increasing non-stoichiometry of the $Ni_{1-x}S$ phase on the sulfur-rich side. Accordingly, the exsolution of small amounts of $Ni_{3\pm x}S_2$ phase occurs during sample preparation at about 1270 K and might not be reversed completely on cooling. Thereby a slightly nickel-deficient NiAs-type $Ni_{1-x}S$ is formed, which disproportionates into a two-phase mixture of NiS (millerite) and Ni_3S_4 (polydymite). Furthermore, the coexisting NiS phases have, in principle, different compositions. If the NiAs-type phase has the slightly higher sulfur content, as indicated in Fig. 4, a small amount of Ni_3S_4 should precipitate below the eutectoid temperature, 555 K [5], for the coexistence of NiS, $Ni_{1-x}S$ and Ni_3S_4. If some of this Ni_3S_4 remains during the heat capacity determinations to slightly above 600 K, the small heat capacity maximum in the 610–620 K region might be due to its decomposition. Another possible cause is that some structural order–disorder process occurs in the $Ni_{1-x}S$ phase. In either case the difference between the results for sample A (detn. A) and sample B (detn. B) may be attributed to slight differences in phase composition.

3.2.3. The exothermal NiAs–type to millerite transition

At around 330 K, extra-instrumental drift is observed. Further energy inputs cause the transition to proceed faster. The temperature of the sample is shown as a function of

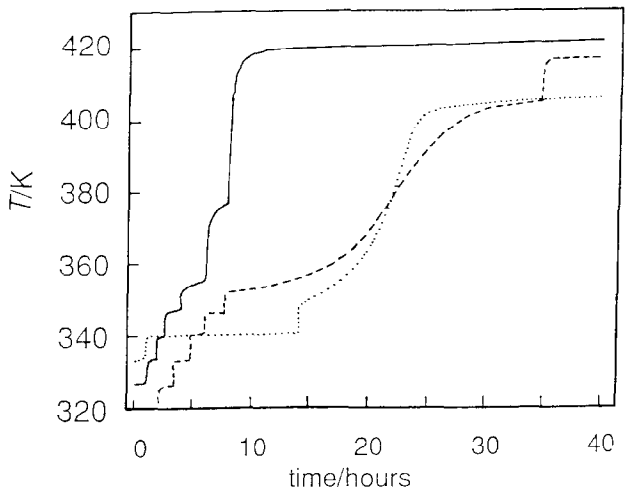

Fig. 5. Temperature vs. time relationship for NiS samples transforming from the NiAs-type to millerite: —, detn. D; ···, detn. F; —, detn. H.

time in Fig. 5. Vertical segments in the figure represent energy input periods of approximately 20 min duration. The combined heating and self-heating raised the calorimeter temperature to above 400 K in a matter of 8–40 h. Three series of experiments (detns. D, F, and H) gave $\Delta_{trs}H_m = -1767$, -1816, and -1790 J mol^{-1} for the transformation of the NiAs-type NiS at 340 K to millerite at 420 K. The derived mean molar isothermal enthalpy decrement for the reaction at 340 K is then $\Delta_{trs}H_m = -5774 \pm 50$ J mol^{-1}.

3.3. Thermodynamic properties

The experimental heat capacities were fitted to polynomials in temperature by the methods of least squares. The enthalpy and entropy values were evaluated by integrating the heat capacity polynomials to the transitional temperatures and adding the transitional enthalpies and entropies at the appropriate temperatures. The standard deviation for the 4-term polynomial expression for millerite up to 600 K is 0.28%, while that for the NiAs-type phase is 0.68% for a 5-term expression from 687 to 991 K.

The thermodynamic properties of NiS in the stable structures are given in Table 5 with inclusion of the molar enthalpy and entropy values for millerite at 298.15 K, taken from Weller and Kelley [23]. The values given for millerite above 600 K do not include the pretransitional component. It can, if necessary, be added in from the results in Table 3 and subtracted from the transitional values added in here at the peak temperature, 660 K. Since the enthalpy and entropy increments were derived separately, a slight mismatch occurs in the Gibbs energy values at the actual transition temperature. We prefer this approach rather than selecting an artificial, lower transi-

tion temperature at which $\Delta_{trs}G_m = 0$. The function values for the NiAs-type phase in the 660–680 K region are similarly affected.

The presently obtained enthalpy increment from 300 to 1000 K is 6.7% larger than the one by Conard et al. [28] in spite of the approximately correct transitional enthalpy in their measurements. The result by Ferrante [29] is even lower than the one by Conard et al. [28] over the same region due to the erroneously small transitional enthalpy observed.

For the NiAs-type NiS, which transforms from the antiferromagnetic (semimetal) to the metallic type at 270 K, thermodynamic values relative to 298.15 K are given in Table 6. The heat capacity values have been interpolated over the region 340–660 K using the following 3-term polynomial

$$C_{p,m} = 46.676 + 0.0199807(T/\mathrm{K}) - 0.2554994 \times 10^6 (\mathrm{K}/T)^2$$

The derived enthalpy increment $\Delta_{340}^{660}H_m = 17769\ \mathrm{J\ mol^{-1}}$ may be compared with the sum of the NiAs-type to millerite transitional enthalpy decrement plus the enthalpy

Table 6
Molar thermodynamic properties of metastable NiAs-type nickel(II) sulfide

T/K	$C_{p,m}$/(J K^{-1} mol^{-1})	$\Delta_{278}^{T}H_m$/(J mol^{-1})	$\Delta_{298}^{T}S_m$/(J K^{-1} mol^{-1})
		M (NiS) = 90.759 g mol^{-1}	
		Non-metallic (observed)	
260	46.50	−3246	−11.81
270	47.00	−2778	−10.04
		Metallic (observed)	
270	48.57	−1384	−4.86
280	49.01	−896	−3.10
298.15	49.76	0.0	0.0
300	49.83	92	0.31
320	50.57	1096	3.55
340	51.26	2115	6.64
		Metallic (estimated)	
360	51.90	3146	9.58
380	52.50	4190	12.41
400	53.07	5246	15.11
420	53.62	6313	17.72
440	54.15	7391	20.22
460	54.66	8479	22.64
480	55.16	9577	24.98
500	55.64	10685	27.24
520	56.12	11803	29.43
540	56.59	12930	31.56
560	57.05	14066	33.62
580	57.51	15212	35.63
600	57.95	16366	37.59
620	58.40	17530	39.50
640	58.84	18702	41.36
660	59.28	19884	43.18

increment for millerite over the same temperature region and the transitional enthalpy from millerite to NiAs-types NiS, i.e. $(-5774 + 16954 + 6591)$ J mol^{-1}. The closeness of the two values indicates that no measurable transition occurs in NiAs-type NiS between 340 and 660 K. This result agrees with the conclusion by White and Mott [17] that the transition from the antiferromagnetic to paramagnetic state presumably does not occur below 1000 K.

Applying the low-temperature results for the antiferromagnetic (AF) and metallic (M) NiAs-type phases reported by Coey and Brusetti [18] and Brusetti et al. [19], enthalpy cycles involving the different NiS phases may be considered. From 0 to 270 K, the approximate enthalpy increments derived here are 7950 and 8550 J mol^{-1} for AF and M, respectively.

If we now consider an enthalpy cycle involving millerite and the metallic NiAs-type NiS between $T = 0$ and 660 K, the enthalpy increment in favor of the latter is 2283 J mol^{-1}. With the enthalpy of transition of millerite to the NiAs-type phase being $\Delta_{trs}H_m = 6591$ J mol^{-1}, the enthalpy of the metallic NiAs-type phase is more positive than millerite by 4308 J mol^{-1} at 0 K. Since the lattice enthalpy difference between metallic and antiferromagnetic NiS, as estimated from the difference in their Debye temperatures, is of the order of 800 J mol^{-1}, while the transition enthalpy is 1400 J mol^{-1}, the latter phase becomes 600 J mol^{-1} more stable at 0 K.

The relative stabilities of the different NiS phases are shown as a function of temperature in Fig. 6 for $p = 0.1$ MPa. The Gibbs energy of formation of the stable

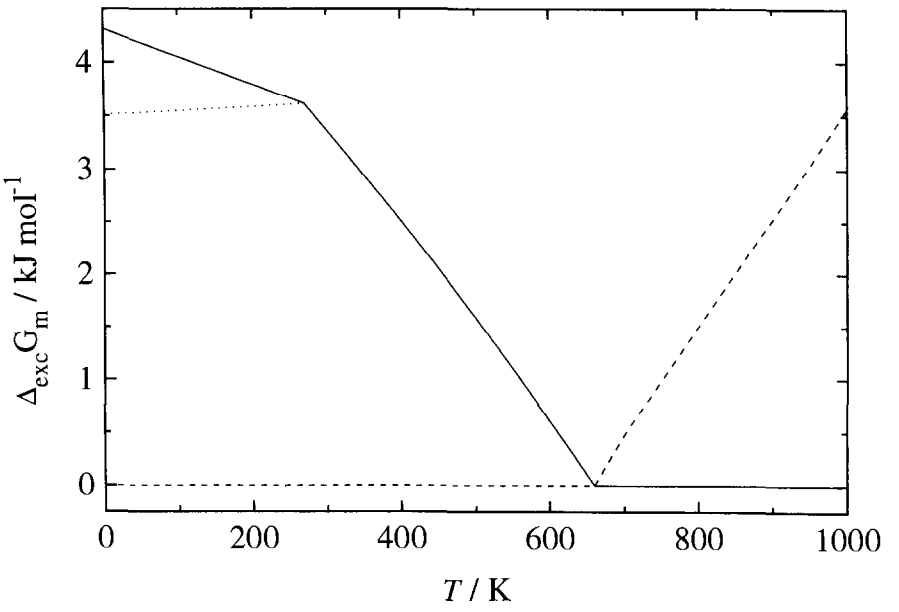

Fig. 6. Excess Gibbs energies for the NiS phases relative to the phase stable in the range 0–1000 K: – – –, millerite; ——, metallic NiAs-type phase; ···; semimetallic NiAs-type phase.

phase is taken as zero at all temperatures. With an approximately linear heat capacity extrapolation to 67 J K^{-1} mol^{-1} at 1000 K for the millerite phase, it becomes increasingly more unstable relative to the metallic NiAs-type phase above 660 K. Conversely, the latter becomes more unstable relative to millerite below 660 K. Finally, below 270 K the metallic phase also becomes unstable relative to the semimetallic NiAs-type phase.

References

[1] N. Alsén, Geol. Fören. Stocken. Förh., 47 (1925) 19.
[2] H.W. Willems, Physica, 7 (1927) 203.
[3] N.H. Kolkmeijer and A.L. Th. Moesveld, Z. Krist., 80 (1931) 91.
[4] W. Biltz, A. Voigt, K. Meisel, F. Weibke and P. Ehrlich, Z. Anorg. Allg. Chem., 228 (1936) 275.
[5] G. Kullerud and R.A. Yund, J. Petrol., 36 (1962) 126.
[6] M. Dubusc, Y. Claire and J. Rey, C.R. Acad. Sci. Paris, 290 (1980) 89.
[7] M. Laffitte, Bull. Soc. Chim. Fr., 7–8 (1959) 1211.
[8] H. Rau, J. Phys. Chem. Solids, 36 (1975) 1199.
[9] R.Y. Lin, D.C. Hu and Y.A. Chang, Metall. Trans., 9B (1978) 531.
[10] C.A. Francis and J.R. Craig, Geol. Soc. Am. Abstr. Progr., 8 (1976) 176.
[11] T. Noda, S. Ohtomo, K. Igaki and W.T. Holser, Trans. Jpn. Inst. Met., 20 (1979) 89.
[12] G. Collin, G. Chavant and F. Keller-Besrest, Bull. Mineral., 103 (1980) 380.
[13] G. Collin, T. Chavant and R. Comes, Acta Crystallogr. Sect. B, 39 (1983) 289.
[14] S.N. Black, D.A. Jefferson and P.J. Henderson, J. Solid State Chem., 53 (1984) 76.
[15] J.T. Sparks and T. Komoto, Phys. Lett., 25 (1967) 398.
[16] R.F. Koehler, Jr., R.S. Feigelson, H.W. Swarts and R.L. White, J. Appl. Phys., 43 (1972) 3127.
[17] R.M. White and N.F. Mott, Phil. Mag., 24 (1971) 845.
[18] J.M.D. Coey and R. Brusetti, Phys. Rev., 11B (1975) 671.
[19] R. Brusetti, J.M.D. Coey, G. Czjzek, F. Fink, F. Gompf and H. Schmidt, J. Phys. F: Metal Phys., 10 (1980) 33, and personal communication.
[20] G.A. Briggs, C. Duffil, M.T. Hutchings, R.D. Lowde, N.S. Satya-Murty, D.H. Saunderson, M.W. Stringfellow, W.B. Waeber and C.G. Windsor, Neutron Inelastic Scattering, Vienna: IAEA, 1972, p. 669.
[21] Z. Anzai and K. Ozawa, J. Appl. Phys., 48 (1977) 2139.
[22] T. Othani, J. Phys. Soc. Jpn., 37 (1974) 701.
[23] W.W. Weller and K.K. Kelley, US Bureau of Mines Report of Investigation 6511, Washington, D.C., 1964.
[24] J. Trahan and R.G. Goodrich, Phys. Rev., 6B (1972) 199.
[25] T. Ohtani, K. Adachi, K. Kosuge and S. Kachi, Phys. Soc. Jpn., 36 (1974) 1489.
[26] V. Regnault, Ann. Chim. Phys., 3(1) (1841) 129; see also Ann. Phys., 53 (1841) 60.
[27] W.A. Tilden, Phil. Trans. R. Soc. London, 201 (1903) 37; see also Proc. R. Soc. London, 71 (1903) 220 for identical results.
[28] B.B. Conard, R. Sridhar and J.S. Warner, Paper presented at the 106th AIME Annual Meeting, Atlanta, Georgia, March 7–11, 1977.
[29] A.D. Mah and L.B. Pankratz, Contribution to the Data on Theoretical Metallurgy. XVI, U.S. Bureau of Mines Bulletin 668, Washington, D.C., 1976.
[30] R.C. Sharma and Y.A. Chang, Metall. Trans., 11B (1980) 139.
[31] M. Singleton, P. Nash and K.J. Lee, Phase Diagrams of Binary Nickel Alloys, ASM International, Metals Park, Ohio, 1991, p. 277.
[32] S. Stølen and F. Grønvold, High Temp. - High Press., 25 (1993) 161.
[33] S. Stølen, F. Grønvold, E.F. Westrum, Jr., and G.R. Kolonin, J. Chem. Thermodyn., 23 (1991) 77.
[34] S. Stølen, H. Fjellvåg, F. Grønvold, H. Seim and E.F. Westrum, Jr., J. Chem. Thermodyn., 26 (1994) 987.

[35] H. Seim, H. Fjellvåg, F. Grønvold and S. Stølen, in preparation
[36] D. Lundqvist, Ark. Kemi Mineral. Geol., 24A (1947) 12.
[37] G. Trahan, R.G. Goodrich and S.F. Watkins, Phys. Rev., B2 (1970) 2859.
[38] D.B. McWhan, M. Marezio, J.P. Remeika and P.D. Dernier, Phys. Rev., B5 (1972) 2352.
[39] E. Barthelemy, C. Charant, G. Collin and O. Gorochov, J. Phys. Paris Colloq., 4 (1976) 17.
[40] F. Grønvold, Acta Chem. Scand., 21 (1967) 1695.
[41] F. Grønvold, J. Chem. Thermodyn., 25 (1993).
[42] F. Grønvold, S. Stølen, P. Tolmach and E.F. Westrum, Jr., J. Chem. Thermodyn., 25 (1994) 1089.
[43] K.K. Kelley, Contributions to the Data on Theoretical Metallurgy. XIII, US Bureau of Mines Bull. 584, Washington, D.C. 1960.
[44] R.F. Koehler, Jr. and R.L. White, J. Appl. Phys., 44 (1973) 1682.
[45] J.T. Sparks and T. Komoto, J. Appl. Phys., 34 (1963) 1191.
[46] T. Rosenqvist, J. Iron Steel Inst., 176 (1954) 37.